



## A Computational Analysis on Thermo-viscous Steady Flow between Extremely Stretched Impervious Parallel Flat Plates

B. Vasu, N. Pothanna, B. Hari Prasad\* and A. Raju

**ABSTRACT:** A computational analysis on steady thermo-viscous flow between extremely stretched impervious parallel flat plates is explored in the current investigation. The governing non-linear coupled differential equations obtained in terms of velocity and temperature are reduced to the non-dimensional form. The `bvp5c` Matlab software tool with collocation techniques has been implemented to solve the resulting fundamental non-dimensional equations governed by the flow. To guarantee accuracy, the solver used an adaptive mesh refinement technique with both absolute and relative tolerances. Mesh independence tests and residual checks were used to confirm numerical convergence. The numerical results obtained are shown in form of tables and graphically depicted for numerous physical factor values of viscosity coefficient, constant pressure, temperature gradients, Prandtl number, conductivity and thermo stress factor's. When the numerical findings are compared to previously known analytical data, it is found that both good concurrence and excellent convergence have been attained.

**Keywords:** Thermo-viscous, `bvp5c`, thermal conductivity, thermo stress coefficient.

### Contents

<b>1 Introduction</b>	<b>1</b>
<b>2 Mathematical Modeling</b>	<b>2</b>
<b>3 Numerical Study</b>	<b>3</b>
<b>4 Comparison of Existing Analytical Results with Numerical Solutions</b>	<b>4</b>
<b>5 Discussion of Results</b>	<b>5</b>
<b>6 Conclusions</b>	<b>10</b>

### 1. Introduction

Non-Newtonian fluid properties have been the focus of extensive research for centuries. However, the attempts have been made on this extensive research to cover the assessments into the principles of non-linear study directed in the recent eight to nine decades. Preliminary work on developing a non-linear paradigm that captures the interaction and relationship between viscous and thermal impacts has been conducted by Koh and Eringen [1]. Rao and Acharyulu [2] assessed the steady 2nd order problem of fluids through an infinite elongated surface. Pothanna [3] used an analytical and numerical method to study an unsteady flow around a fluctuating sphere. The Casson MHD nanofluid and the impact of thermal emission with the presence of chemical reaction on the flow via non-linear elongating sheet was described by Shekar et al. [4]. Using artificial neural networks, Pothanna et al. [5] investigated instable thermos viscous liquid transport among two indefinitely stretched impervious straight plates. Nalimela et al. [6] used artificial neural network techniques to forecast and assess an instable liquid flow over a horizontal oscillating plate in an absorbent slab. Helfrich KR et al. [7] was studied and model a magma flow fingering thermo-viscous liquids with a narrow gap in fissures and dikes. Kulikov et al. [8] was examined the high temperature gradients stability of fluid flows. Kuleshov et al. [9] explored the convective flows of anomalous thermoviscous fluid. Taylor-West et al. [10] explained thermoviscous localization of volcanic explosions is improved by changes in the fracture width. Balaji et al. [11] discovered a destabilization and stabilization of network flows by viscosity-laminated fluid layer location. Weiming et al. [12] explored

\* Corresponding author.

2020 *Mathematics Subject Classification*: 58D30, 76A05, 35Q30.

Submitted March 04, 2026. Published June 19, 2026.

the linear stability of thermal layered rotary network flow. Leblanc and Cambon et al. [13] examined the 3D uncertainties of simple flows exposed to coriolis force. Sparrow et al. [14] presented the problem of wide-gap instability of the flow between circulating cylinders. Aouidef et al. [15] studied coriolis impacts on gortler storms in the boundary surface flow on wall concavity. Pothanna et al. [16] examined steady flow of fluid between two flat plane plates with upper plate in relative movement using analytical and numerical approach. Shah et al. [17] invented mhd with porous influences on viscous free convective flow between perpendicular flat plates. This work studied advanced thermal investigation on the flow behaviour. The thermodynamical ternary nanofluid activity of a flow via a pervious sliding surface with a sink and heat source was investigated by Ramesh et al. [18]. Thermal transportation of magnetic nano particles through a greased surfaces with activation energy, sink and heat source was investigated by Ramesh et al. [19]. The computational investigation and simulation for squeezing blood dependent hybrid nanofluid through two pervious shells under mhd and viscous dissipation influence was found by Ali Rehman et al. [20]. The heat and mass transfer behavior of a 2 dimensional forch-heimer absorbent medium on casson mhd fluid through an oriented surface with dissipation, chemical effect etc. was examined by Kumar et al. [21].

The current work aims to investigate a computational analysis on steady thermo-viscous flow between extremely stretched impervious parallel flat plates, taking into account the rising interest and applications of non-Newtonian type flow in an industry, chemical field and geothermal flow dynamics. The obtained results of leading equations are also portrayed in the form of tables and the influence of several material factors of the problem is examined and described with different mathematical values. There has been a important flow in attention over the last several decades in studying the flow characteristics in these arrangements, driven by the wide array of applications.

In this work, the consequences of different material characteristics on thermo-viscous flow between extremely stretched impervious parallel flat plates are attempted to be studied. The constituent concepts mentioned so far have not taken into justification of this computational analysis using collocation based bvp5c method.

## 2. Mathematical Modeling

Consider the steady flow between two impervious flat plates as shown in Figure 1. The upper plate's movement in the flow direction at a particular speed relative to the lower plate is investigated. The plates are represented with  $y = 0$  and  $y = h$  in the coordinate system  $O(XYZ)$ . The origin is on the stationary plate, the  $y$ -axis is orthogonal to the plates, and the  $x$ -axis points are considered in the plate movement direction. Additionally, the two plates are kept at a constant temperatures.

Consider  $[u(y), 0, 0]$  as the velocity and  $\theta(y)$  as the temperature defined for the steady flow through the flat plates parallel to each other. The mass conservation equation is verified with this choosing of velocity.

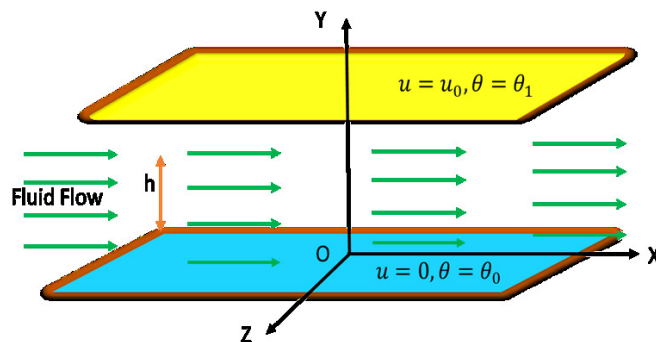


Figure 1: Flow Configuration

The basic equations which described as follows:

Along the X-direction:

$$0 = -\frac{\partial p}{\partial x} + \mu \frac{\partial^2 u}{\partial y^2} - \alpha_6 \frac{\partial \theta}{\partial x} \frac{\partial^2 \theta}{\partial y^2} + \rho F_x \quad (2.1)$$

Along the Y-direction:

$$0 = \mu_c \frac{\partial}{\partial y} \left( \frac{\partial u}{\partial y} \right)^2 + \rho F_y \quad (2.2)$$

Along the Z- direction:

$$0 = \alpha_8 \frac{\partial}{\partial y} \left( \frac{\partial \theta}{\partial y} \frac{\partial u}{\partial y} \right) + \rho F_z \quad (2.3)$$

and the heat equation as

$$\rho c \left( u \frac{\partial \theta}{\partial x} \right) = \mu \left( \frac{\partial u}{\partial y} \right)^2 - \alpha_6 \frac{\partial \theta}{\partial x} \frac{\partial u}{\partial y} \frac{\partial \theta}{\partial y} + k \frac{\partial^2 \theta}{\partial y^2} + \beta_3 \frac{\partial \theta}{\partial x} \frac{\partial^2 u}{\partial y^2} + \rho \gamma \quad (2.4)$$

along the boundary limitations:

$$u = 0, \theta = \theta_0 \text{ when } y = 0 \text{ and } u = u_0, \theta = \theta_1 \text{ when } y = h \quad (2.5)$$

With the inclusion of these dimensionless quantities:

$$y = hY, u = \left( \frac{\mu}{\rho h} \right) U, u_0 = \left( \frac{\mu}{\rho h} \right) U_0, T = \frac{\theta - \theta_0}{\theta_1 - \theta_0}, \frac{\partial \theta}{\partial x} = \frac{\theta_1 - \theta_0}{h} C_2, \frac{\partial p}{\partial x} = \frac{\mu^2}{\rho h^3} C_1,$$

$$p_r = \frac{\mu c}{k} \text{ (Prandtle number)}, b_3 = \frac{\beta_3}{\rho h^2 c} \text{ and } a_6 = \frac{\alpha_6 \rho (\theta_1 - \theta_0)^2}{\mu^2}$$

Where dimensionless constant pressure and temperature gradients are  $C_1$  and  $C_2$  correspondingly. The external forces, and internal heat sources are eliminated and the abovementioned following non-dimensional equations (2.6) and (2.7) can be solved with respect to the boundary conditions (2.8) and (2.9) employing the BVP5C method.

along the X-direction :

$$0 = -C_1 + \mu \frac{d^2 U}{dY^2} - a_6 C_2 \frac{d^2 T}{dY^2} \quad (2.6)$$

and energy equation is

$$\rho c U C_2 = a_1 \left[ \left( \frac{dU}{dY} \right)^2 - a_6 C_2 \frac{dU}{dY} \frac{dT}{dY} \right] + \frac{1}{p_r} \frac{d^2 T}{dY^2} + b_3 C_2 \frac{d^2 U}{dY^2} \quad (2.7)$$

along the suitable boundary limits:

$$U(0) = 0, T(0) = 0 \quad (2.8)$$

and

$$U(1) = 1, T(1) = 1 \quad (2.9)$$

where  $a_1 = \frac{\mu^2}{\rho h^2 c (\theta_1 - \theta_0)}$

### 3. Numerical Study

The  $2^{nd}$  order linear ordinary differential equations (2.6) and (2.7) that have been obtained are in terms of velocity and temperature coupled equations. The obtained results of governed equations (2.6) and (2.7) by utilizing the boundary conditions (2.8) and (2.9) for velocity and temperature were measured using the MATLAB software `bvp5c` tool with collocation method along with the shooting approach. To facilitate numerical computation, the equations were converted to a first-order system of equations. The solver employed an adaptive mesh refinement strategy to ensure accuracy, with relative and absolute

tolerances. The distance between the plates were denoted with the unit " $h$ " and has been converted to a finite value of 1 once dimensional-less values were included into the fluid equations. Numerical convergence was verified through residual checks and mesh independence tests, while solutions were cross-validated against analytical benchmarks where applicable. The resulting velocity ( $U$ ) and temperature ( $T$ ) profiles was analyzed parametrically, demonstrating the method's robustness in handling nonlinear fluid-thermal interactions. This approach provides an efficient and reliable framework for solving such coupled boundary value problems. The convergence of the solution was ensured by meeting the boundary constraints of the issue. To demonstrate how various material constants affect the fluid's temperature and velocity, tables and images have been used.

Tables 1 and 2 present the numerical results related to the different material quantities and give the fluid governing equation solutions attributable to temperature and velocity. The `bvp5c` tool in MATLAB has generated the numerical computations of the equations that govern (2.6) and (2.7) concerning the boundary conditions (2.8) and (2.9).

Table 1: Computations of the velocity profiles

Y	Velocity U(Y)								
	$b_3 = 1$			$b_3 = 3$			$b_3 = 5$		
	$a_1 = 1$	$a_1 = 2$	$a_1 = 3$	$a_1 = 1$	$a_1 = 2$	$a_1 = 3$	$a_1 = 1$	$a_1 = 2$	$a_1 = 3$
0.0	0.0000	0.0000	0.0000	0.0000	0.0000	0.0000	0.0000	0.0000	0.0000
0.1	0.0092	0.0206	0.0320	0.0375	0.0447	0.0540	0.0516	0.0572	0.0652
0.2	0.0409	0.0672	0.0941	0.0928	0.1121	0.1342	0.1183	0.1340	0.1525
0.3	0.0963	0.1400	0.1835	0.1657	0.1992	0.2331	0.1990	0.2262	0.2533
0.4	0.1749	0.2357	0.2923	0.2549	0.3010	0.3419	0.2921	0.3289	0.3603
0.5	0.2751	0.3486	0.4117	0.3581	0.4121	0.4545	0.3955	0.4377	0.4694
0.6	0.3944	0.4729	0.5347	0.4728	0.5282	0.5674	0.5070	0.5496	0.5783
0.7	0.5295	0.6033	0.6569	0.5963	0.6465	0.6790	0.6247	0.6626	0.6861
0.8	0.6774	0.7362	0.7759	0.7266	0.7652	0.7885	0.7469	0.7758	0.7924
0.9	0.8351	0.8689	0.8904	0.8616	0.8832	0.8955	0.8723	0.8883	0.8971
1.0	1.0000	1.0000	1.0000	1.0000	1.0000	1.0000	1.0000	1.0000	1.0000

Table 2: Computations of the temperature profiles

Y	Temperature T(Y)								
	$b_3 = 1$			$b_3 = 3$			$b_3 = 5$		
	$a_1 = 1$	$a_1 = 2$	$a_1 = 3$	$a_1 = 1$	$a_1 = 2$	$a_1 = 3$	$a_1 = 1$	$a_1 = 2$	$a_1 = 3$
0.0	0.0000	0.0000	0.0000	0.0000	0.0000	0.0000	0.0000	0.0000	0.0000
0.1	1.4845	1.4236	1.3625	2.8339	2.6210	2.3484	3.5792	3.2821	2.8539
0.2	2.6485	2.5084	2.3645	4.9449	4.3795	3.7288	6.1584	5.3209	4.3324
0.3	3.4866	3.2533	3.0211	6.3393	5.3570	4.3625	7.7870	6.3342	4.8914
0.4	4.0006	3.6765	3.3743	7.0571	5.7046	4.5043	8.5551	6.5908	4.9161
0.5	4.1993	3.8074	3.4710	7.1629	5.5793	4.3347	8.5748	6.3215	4.6340
0.6	4.0966	3.6781	3.3482	6.7324	5.1060	3.9550	7.9610	5.6882	4.1584
0.7	3.7091	3.3156	3.0298	5.8407	4.3695	3.4150	6.8184	4.7923	3.5408
0.8	3.0537	2.7403	2.5286	4.5540	3.4219	2.7372	5.2344	3.6929	2.8035
0.9	2.1462	1.9657	1.8512	2.9265	2.2932	1.9311	3.2777	2.4229	1.9555
1.0	1.0000	1.0000	1.0000	1.0000	1.0000	1.0000	1.0000	1.0000	1.0000

#### 4. Comparison of Existing Analytical Results with Numerical Solutions

The corresponding numerical values of the already current existing analytical outcomes for the related governing equations of motion (2.6) and (2.7), along with the boundary conditions (8 and 9), have been

found in terms of  $U(Y)$  and  $T(Y)$ . The MATLAB code has developed and executed in order to acquire the most existing analytical values of equations (2.6) and (2.7) for the temperature and velocity for several values of physical properties. Excellent convergence was achieved between the analytical responses and the numerical results as seen in table 3 and table 4. The obtained closed form results conform the consistency and accuracy of the present study’s numerical findings.

Table 3: Comparison of velocity profile results

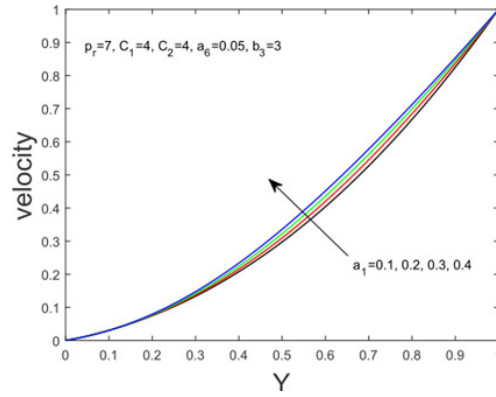
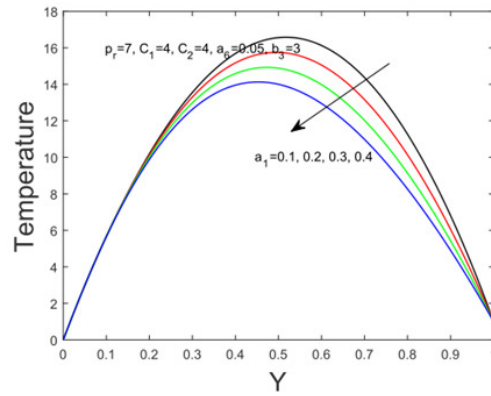
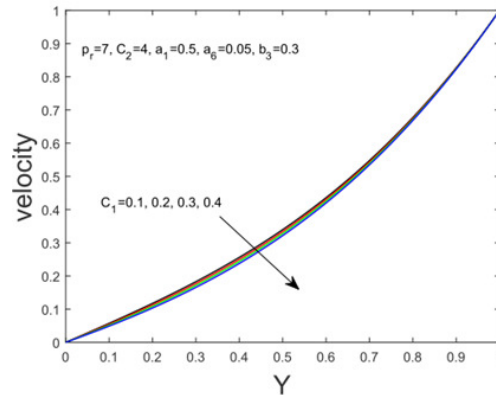
Y	Numerical Results for $b_3 = 3$		Analytical Results of Pothanna <i>et al.</i> [16] with $S = 0$		Numerical Results for $b_3 = 5$		Analytical Results of Pothanna <i>et al.</i> [16] with $S = 0$	
	$a_1 = 1$	$a_1 = 2$	$a_1 = 1$	$a_1 = 2$	$a_1 = 1$	$a_1 = 2$	$a_1 = 1$	$a_1 = 2$
0.0	0.0000	0.0000	0.0000	0.0000	0.0000	0.0000	0.0000	0.0000
0.1	2.8339	2.6210	2.8340	2.6209	0.0516	0.0572	0.0517	0.0573
0.2	4.9449	4.3795	4.9450	4.3800	0.1183	0.1340	0.1184	0.1339
0.3	6.3393	5.3570	6.3394	5.3569	0.1990	0.2262	0.1989	0.2263
0.4	7.0571	5.7046	7.0569	5.7047	0.2921	0.3289	0.2919	0.3290
0.5	7.1629	5.5793	7.1630	5.5794	0.3955	0.4377	0.3956	0.4378
0.6	6.7324	5.1060	6.7322	5.1059	0.5070	0.5496	0.5069	0.5497
0.7	5.8407	4.3695	5.8400	4.3696	0.6247	0.6626	0.6248	0.6627
0.8	4.5540	3.4219	4.5539	3.4220	0.7469	0.7758	0.7470	0.7760
0.9	2.9265	2.2932	2.9264	2.29321	0.8723	0.8883	0.8724	0.8884
1.0	1.0000	1.0000	1.0000	1.0000	1.0000	1.0000	1.0000	1.0000

Table 4: Temperature profile results comparison

Y	Numerical Results for $b_3 = 3$		Analytical Results of Pothanna <i>et al.</i> [16] with $S = 0$		Numerical Results for $b_3 = 5$		Analytical Results of Pothanna <i>et al.</i> [16] with $S = 0$	
	$a_1 = 1$	$a_1 = 2$	$a_1 = 1$	$a_1 = 2$	$a_1 = 1$	$a_1 = 2$	$a_1 = 1$	$a_1 = 2$
0.0	0.0000	0.0000	0.0000	0.0000	0.0000	0.0000	0.0000	0.0000
0.1	2.8339	2.6210	2.8340	2.6209	3.5792	3.2821	3.5790	3.2819
0.2	4.9449	4.3795	4.9451	4.3796	6.1584	5.3209	6.1585	5.3208
0.3	6.3393	5.3570	6.3390	5.3569	7.7870	6.3342	7.7869	6.3341
0.4	7.0571	5.7046	7.0572	5.7047	8.5551	6.5908	8.5549	6.5909
0.5	7.1629	5.5793	7.1632	5.5794	8.5748	6.3215	8.5750	6.3213
0.6	6.7324	5.1060	6.7325	5.1059	7.9610	5.6882	7.9611	5.6881
0.7	5.8407	4.3695	5.8405	4.3696	6.8184	4.7923	6.8183	4.7924
0.8	4.5540	3.4219	4.5539	3.4220	5.2344	3.6929	5.2343	3.6930
0.9	2.9265	2.2932	2.9264	2.2931	3.2777	2.4229	3.2778	2.4232
1.0	1.0000	1.0000	1.0000	1.0000	1.0000	1.0000	1.0000	1.0000

### 5. Discussion of Results

The numerical results are depicted and graphically represented in Figs. 2–13, was conducted using the numerical results that were obtained by developing the code using the bvp5c tool in MATLAB. This predicts how the existing results in the literature are well agreement with the present results. Examining the  $U(Y)$  and  $T(Y)$  field findings revealed the physical impression of the issue, which were produced by assigning numerous estimations to various physical quantities such as constant pressure gradient ( $C_1$ ) and temperature gradient ( $C_2$ ) values including the stress coefficient ( $a_6$ ), conductivity coefficient ( $b_3$ ) and prandtl parameter ( $p_r$ ) values which relates to fixed values like density ( $\rho$ ), viscosity ( $\mu$ ), the specific heat ( $c$ ) etc. To demonstrate how each of these factors affects the  $U(Y)$  and  $T(Y)$  fields, the graphical representations have been presented.

Figure 2: Velocity variations vs.  $(a_1)$ Figure 3: Temperature variations vs.  $(a_1)$ Figure 4: Velocity variations vs.  $(C_1)$ .

The variations of  $U(Y)$  and  $T(Y)$  fields have been studied with respect to  $(a_1)$  and illustrated graphically in Figure 2 and Figure 3. It is clearly noticed that, velocity variations are less near the lower and upper plate boundaries and little bit more in the middle flow zone. It is found that from Figure 2 that, velocity profiles decrease as the values of  $(a_1)$  increase from  $(a_1)=0.1$  to 0.4. Figure 3 shows that, temperature of the fluid increase up to centre profile region and then decreases to realise the upper flat plate limit. Completely opposite variations have been seen with increase of  $(a_1)$  on  $U(Y)$  and  $T(Y)$

profiles.

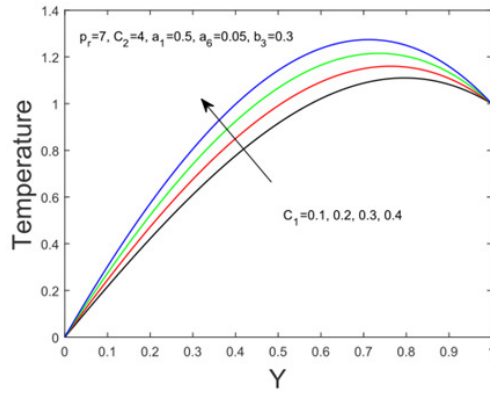


Figure 5: Temperature variations vs.  $(C_1)$

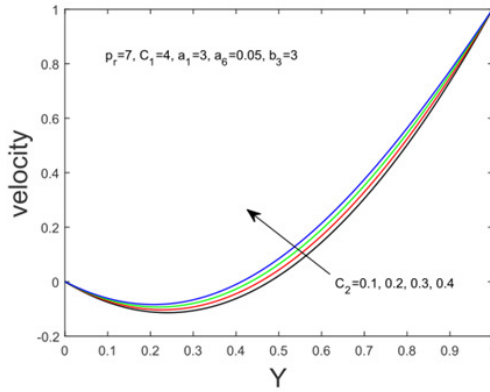


Figure 6: Velocity variations vs.  $(C_2)$ .

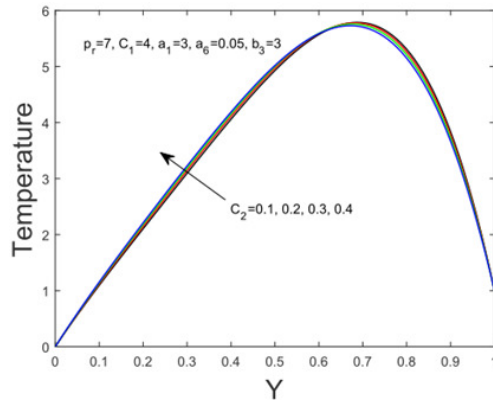


Figure 7: Temperature variations vs.  $(C_2)$ .

The changes in the  $U(Y)$  and  $T(Y)$  fields profiles are studied with respect to  $(C_1)$  and illustrated graphically in Figure 4 and Figure 5. It is discussed from the Figure 4 that, the velocity profiles decrease with smaller rate as the values of  $(C_1)$  increase from  $(C_1)=0.1$  to 0.4. Figure 5 shows that, temperature

of the fluid increases near to the hooter plate region and then decreases to reach the upper plate limit. The variations of temperature profiles have been seen to be increase increase with increase of ( $C_1$ ) values.

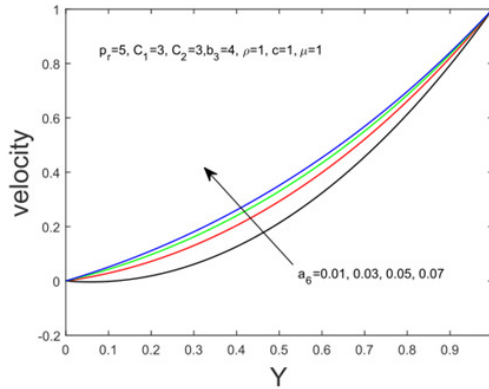


Figure 8: Velocity variations vs. ( $a_6$ ).

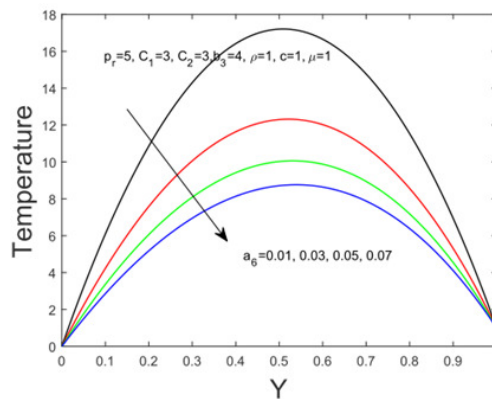


Figure 9: Temperature variations vs. ( $a_6$ ).

The  $U(Y)$  and  $T(Y)$  fields variations are studied with respect to ( $C_2$ ) and illustrated graphically in Figure 6 and Figure 7. As shown in Figure 6, the velocity of the fluid deviates to the negative flow area near the lower plate and then suddenly takes turn and increases up to the hotter plate. It is also found from the Figure 6 that, the velocity profiles are increases as ( $C_2$ ) increases from 0.1 to 0.4. The  $T(Y)$  of the fluid in Figure 7 shows that, it increases near the middle flow region and then reduces to reach the upper plate temperature. It shows that the temperature increases near the middle region and then decreases with the very smaller rate as temperature gradient values increases.

Figure 8 and 9 depicts the the  $U(Y)$  and  $T(Y)$  profiles changes with the small values of the coefficient ( $a_6$ ). The Figure 8 depicts that, the  $U(Y)$  profile deviates to the negative flow region to positive flow region as ( $a_6$ ) increases and it is also observed that it is increases from cooler plate to hotter plate. Figure 9 shows that, the temperature of the fluid increase up to centre flow area and then decreases to reach the hotter plate limit. It shows that the temperature decreases with the faster rate as the ( $a_6$ ) values increases.

The velocity and temperature variations are noted with various ( $b_3$ ) values and illustrated graphically in Figure 10 and Figure 11. As shown in Figure 10, the velocity of the fluid deviates to the lower flow area to the upper flow area as ( $b_3$ ) values increases and it is also observed that, the increasing rate of the fluid is less with respect to the increase of ( $b_3$ ) values. Figure 11 shows that, the temperature of the fluid increase up to middle flow region and then decreases to reach its upper plate boundary limit. It shows

that the temperature increases with the faster rate as small heat conductivity values increases from 0.1 to 0.4.

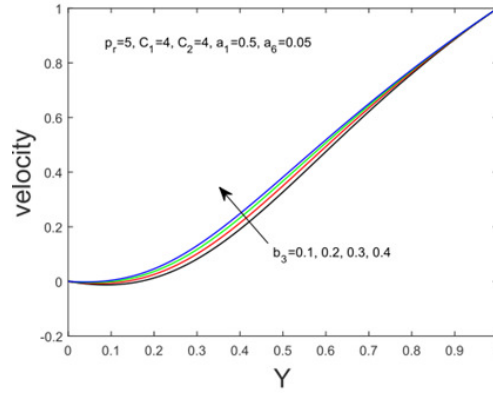


Figure 10: Velocity variations vs. ( $b_3$ ).

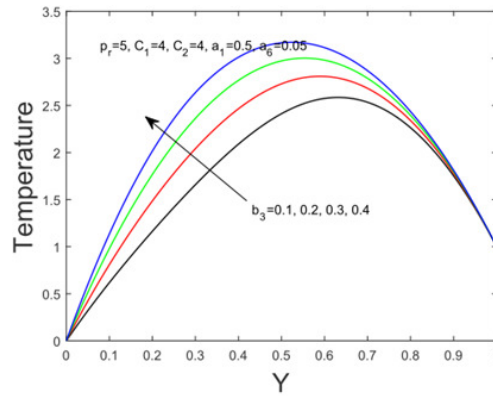


Figure 11: Temperature variations vs. ( $b_3$ ).

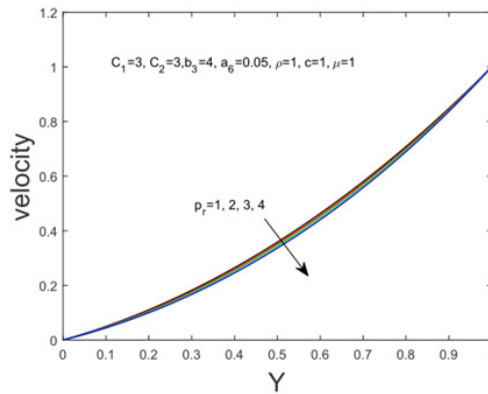


Figure 12: Velocity variations vs. ( $p_r$ ).

The profiles of velocity and temperature changes with the values of ( $p_r$ ) are observed in Figure 12 and 13. Figure 11 shows that, as the ( $p_r$ ) values increases (i.e. from  $p_r = 1 - 4$ ), the velocity field decreases

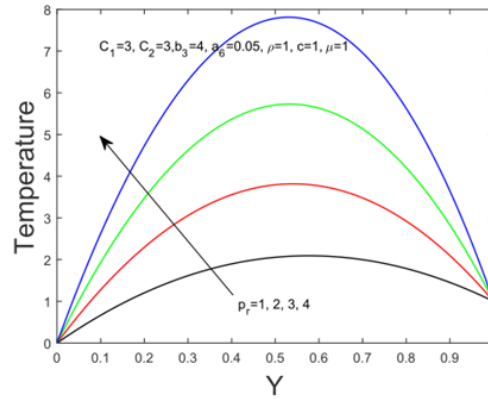


Figure 13: Temperature variations vs.  $(p_r)$ .

with the slow rate and all the profiles almost coincides, where as the temperature of the fluid increases at a greater rate for the values of  $(p_r)$  increases (As observed in Figure 13).

## 6. Conclusions

The present study explores a numerical investigation on the thermo-viscous slow steady flow between horizontally extended no-penetrable flat plates. The governing equations' numerical solution has been found, and the BVP5C tool in MATLAB is utilized to solve the resulting governing equations. For a range of physical values of different parameters, as well as for some fixed values of other coefficients, the solutions are implemented.

1. The fluid's velocity increases and temperature decreases when the small viscosity dependent coefficient  $(a_1)$  values increases.
2. The fluid's velocity reduces with the less rate and temperature increases with the faster rate as  $(C_1)$  values increases.
3. The fluid's velocity increases with the faster rate and temperature increases with the smaller rate as  $(C_2)$  values increases.
4. The fluid's velocity increases and temperature decreases when the small coefficient of thermal stress  $(a_6)$  values increases.
5. The fluid's velocity increases with the smaller rate and temperature increases with the faster rate as  $(b_3)$  rises to small values.
6. The velocity profiles decreases and almost coincides with the raise of  $(p_r)$  values.
7. The fluid temperature rises more and more quickly with rising of prandtl number  $(p_r)$  values.

## References

1. Koh, S. L. and Eringen, A. C., *On the foundations of non-linear thermo-viscoelasticity*, Int. J. Eng. Sci. 1, 199–229, (1963).
2. Rao, P. N. and Pattabhiramacharyulu, N. Ch., *Steady flow of a second-order thermo-viscous fluid over an infinite plate*, Proc. Indian Acad. Sci. Math. Sci. 88, 157–161, (1979).
3. Pothanna, N., *Investigation on unsteady fluid flow around an oscillating sphere—a numerical and analytical approach*, Hybrid Adv. 6, 100257, (2024).
4. Shekar, P. R., Reddy, G. J. and Pothanna, N., *Influence of thermal radiation on MHD Casson nanofluid flow over a non-linear stretching sheet with the presence of chemical reaction*, East Eur. J. Phys. 1, 101–111, (2025).

5. Pothanna, N., Srinivas, J., Thirmal, C., Ramesh Chandra, G. and Sandeep Raj, L., *Unsteady thermo-viscous fluid motion between two infinitely extended impermeable horizontal plates—an artificial neural networks approach*, Therm. Sci. Eng. Prog. 62, 103617, (2025).
6. Nalimela, P., Thirmal, C., Kumar, V. G. and Reddy, G. J., *Artificial neural networks analysis of an unsteady fluid flow through a horizontal oscillating flat plate in a porous slab*, Phys. Fluids 37, (2025).
7. Helfrich, K. R., *Thermo-viscous fingering of flow in a thin gap: a model of magma flow in dikes and fissures*, J. Fluid Mech. 305, 219–238, (1995).
8. Kulikov, Y. M. and Son, E. E., *Stability of thermoviscous fluid flow under high temperature gradients*, High Temp. 55, 131–138, (2017).
9. Kuleshov, V. S., Moiseev, K. V. and Khizbullina, S. F., *Convective flows of anomalous thermoviscous fluid*, Math. Models Comput. Simul. 10, 529–537, (2018).
10. Taylor-West, J. J. and Llewellyn, E. W., *Thermoviscous localisation of volcanic eruptions is enhanced by variations in fissure width*, J. Fluid Mech. 1015, A18, (2025).
11. Ranganathan, B. T. and Govindarajan, R., *Stabilization and destabilization of channel flow by location of viscosity-stratified fluid layer*, Phys. Fluids 13, 1–3, (2001).
12. Sha, W., Tsuchiya, K. and Nakabayashi, K., *The linear stability of thermally stratified rotating channel flow*, Phys. Fluids 11, 439–449, (1999).
13. Leblanc, S. and Cambon, C., *On the three-dimensional instabilities of plane flows subjected to Coriolis force*, Phys. Fluids 9, 1307, (1997).
14. Sparrow, E. M., Munro, W. D. and Jonsson, V. K., *Instability of the flow between rotating cylinders: the wide-gap problem*, J. Fluid Mech. 20, 35–46, (1964).
15. Aouidef, A., Wesfreid, J. E. and Mutabazil, I., *Coriolis effects on Görtler vortices in the boundary-layer flow on concave wall*, AIAA J. 30, 2779–2782, (1992).
16. Pothanna, N., Aparna, P., Sireesha, G. and Padmaja, P., *Analytical and numerical study of steady flow of thermo-viscous fluid between two horizontal parallel plates in relative motion*, Commun. Math. Appl. 13, 1427–1441, (2022).
17. Shah, N. A., Ebaid, A., Oreyeni, T. and Yook, S. J., *MHD and porous effects on free convection flow of viscous fluid between vertical parallel plates: advance thermal analysis*, Waves Random Complex Media, 1–13, (2023).
18. Ramesh, G. K., Madhukesh, J. K., Das, R., Shah, N. A. and Yook, S. J., *Thermodynamic activity of a ternary nanofluid flow passing through a permeable slipped surface with heat source and sink*, Waves Random Complex Media 35, 3499–3519, (2022).
19. Ramesh, G. K., Madhukesh, J. K., Hiremath, P. N. and Roopa, G. S., *Thermal transport of magnetized nanoliquid flow over lubricated surface with activation energy and heat source/sink*, Numer. Heat Transf. B 85, 922–939, (2023).
20. Rehman, A., Saad, A. A., Inc, M. and Sudarmozhi, K., *Mathematical simulation for squeezing blood-based hybrid nanofluid between two permeable surfaces with the influence of MHD and viscous dissipation*, J. Taibah Univ. Sci. 19, (2025).
21. Kumar, M. A., Pothanna, N. and Reddy, G. J., *Analyzing the heat and mass transfer behavior in a 2-D Forchheimer porous medium on MHD Casson fluid flow over an inclined non-linear surface with viscous dissipation, chemical reaction, and Soret–Dufour parameters*, Multiscale Multidiscip. Model. Exp. Des. 8, 176, (2025).

Beeram Vasu,  
 Research Scholar,  
 Chaitanya Deemed to be University,  
 Telangana State, India.  
 E-mail address: vasuharitha9@gmail.com

and

N. Pothanna,  
 Department of Mathematics,  
 VNR Vignana Jyothi Institute of Engineering and Technology,  
 Hyderabad-500090, Telangana State, India.  
 E-mail address: pothanna\_n@vnrvjiet.in

and

Bitla Hari Prasad,

*Department of Mathematics,*  
*Chaitanya Deemed to be University,*  
*Telangana State, India.*  
*E-mail address: sumathi.prasad73@gmail.com*

*and*

*Adigoppula Raju,*  
*Department of Applied Sciences,*  
*Chaitanya Deemed to be University,*  
*Telangana State, India.*  
*E-mail address: rajuardi2013@gmail.com*